Geophysical Research Letters

RESEARCH LETTER
10.1029/2018GL081242

Evaluating Recent Updated Black Carbon Emissions and Revisiting the Direct Radiative Forcing in Arctic

Xinyi Dong[1], Qingzhao Zhu[1], Joshua S. Fu[1,2], Kan Huang[1,3], Jiani Tan[1], and Matthew Tipton[1]

[1]Department of Civil and Environmental Engineering, University of Tennessee, Knoxville, TN, USA, [2]Climate Change Science Institute and Computational Sciences and Engineering Division, Oak Ridge National Laboratory, Oak Ridge, TN, USA, [3]Center for Atmospheric Chemistry Study, Department of Environmental Science and Engineering, Fudan University, Shanghai, China

Key Points:
- Recent updated black carbon (BC) emissions are applied within GEOS-Chem model to estimate BC direct forcing
- FEI-NE may overestimate fire emission over northern Eurasia, probably because of applying the U. S. plant species-based emission factors
- The emission updates are only 10% higher on global scale but are 3 times of the inventory used by IPCC in the Arctic region, leading to substantial enhancement of direct forcing estimation, and indicating the urgent need to further validate and improve these emissions

Correspondence to:
J. S. Fu,
jsfu@utk.edu

Citation:
Dong, X., Zhu, Q., Fu, J. S., Huang, K., Tan, J., & Tipton, M. (2019). Evaluating recent updated black carbon emissions and revisiting the direct radiative forcing in Arctic. *Geophysical Research Letters*, *46*. https://doi.org/10.1029/2018GL081242

Received 7 NOV 2018
Accepted 24 FEB 2019
Accepted article online 27 FEB 2019

Abstract There is significant uncertainty in the global inventory of black carbon (BC). Several recent studies have reported BC emission updates, including the Fire Emission Inventory-northern Eurasia, anthropogenic emission in Russia, and global natural gas flaring. Compared with the inventory used by Intergovernmental Panel on Climate Change, these updates are only 10% higher on a global scale but are 3 times greater than previous estimations in Arctic (60–90°N). We applied GEOS-Chem to examine these emission updates and evaluate their impacts on direct forcing. We found that Fire Emission Inventory-northern Eurasia may be substantially overestimated, Russia shows no prominent influence on simulation, and natural gas flaring noticeably improves simulation performance in the Arctic. Model estimated direct forcing of BC is increased by 30% on the global scale and is 2 times higher in the Arctic through application of these emission updates. This study reveals the urgent need to improve the reliability of emission inventories in the high latitudes, especially over Eurasia.

Plain Language Summary Recent black carbon (BC) emission updates suggest a substantially higher inventory than that used by Intergovernmental Panel on Climate Change. Through GEOS-Chem modeling, we found that the Fire Emission Inventory-northern Eurasia biomass burning emission is overestimated over northern Eurasia, likely due to employment of U.S. plants species-based emission factors. Russian anthropogenic and natural gas flaring inventories help improve simulation performance in the Arctic. Model estimated direct forcing of BC is doubled when applying these emission updates, indicating the urgent need to further validate and improve the BC emission inventory.

1. Introduction

The impact of black carbon (BC) on climate has been extensively investigated during the past decade through various metrics, among which the direct radiative forcing (DRF) and direct radiative effect (DRE) are most frequently applied (Heald et al., 2014). DRE describes the instantaneous influence of BC on the atmospheric energy balance while DRF is calculated as the change of DRE from preindustrial to present day. Despite the tremendous efforts (Huang, Fu, et al., 2015; Huang, Song, et al., 2015; Qi et al., 2017; Samset & Myhre, 2015; Tosca et al., 2013), significant uncertainty remains in the estimation of BC direct forcing (R. Wang et al., 2018). Phase I of the Aerosol Model Comparison Project (Schulz et al., 2006) reported global mean BC DRF between 1750 and 2000 as 0.25 W/m^2 with a range of 0.08 to 0.36 W/m^2. Bond et al. (2013) reported industrial-era (1750–2005) BC DRF as 0.71 W/m^2 with 90% uncertainty bounds of (0.08, 1.27) W/m^2. The Intergovernmental Panel on Climate Change (IPCC) Fifth Assessment Report (AR5) reported BC DRF for 1759–2011 as 0.40 W/m^2 (0.05–0.80) with a medium to low level of scientific understanding. These multimodel assessments reveal large discrepancies in the estimation of BC direct forcing due to diversities in emissions, lifetime, and mass absorption cross section, which is influenced by aerosol refractive index, size, water content, and mixing states with other aerosols. Lifetime and mass absorption cross section varied by a factor of 3 among models (Bond et al., 2013; Huneeus et al., 2011) due to the differences in deposition and aging mechanisms and parameterizations of optical properties. While the emission inventory input should be fairly consistent between models, it contains substantial uncertainties. For example, even with the well-constrained emissions developed though a serious of studies (Bond et al., 2004, 2007), Bond et al. (2013) had to scale the emission by a

factor of 2.9 to match modeled BC aerosol absorbing optical depth (AAOD) with AERONET (AErosol RObotic NETwork) observations.

Due to the diversities of burning activities (e.g., combustion completeness, fuel type, and fuel load) and emission factors, reported BC emission rates from both anthropogenic and biomass burning vary substantially. Arctic Monitoring and Assessment Programme, AMAP (2015) reported that the different anthropogenic emission inventories can vary by a factor of 1.94 for the Northern Hemisphere (NH; 40–90°N), and biomass burning emission can vary by a factor of 1.76 on global scale and 7.48 over the Arctic (north of 60°N). Nevertheless, some inventories have been frequently applied in most of the recent research programs. The inventory promoted by Bond et al. (2007) configured the historical BC inventory and estimated the emission as 4.4 Tg/year from fossil fuel and biofuel for 2000, and the Global Fire Emission Database (GFED) reported the global fire emission since 1997 as 1.6–2.8 Tg/year with timely updates (van der Werf et al., 2017). These two inventories have been applied in the CMIP5 program (Lamarque et al., 2010) in support of IPCC AR5 and other programs such as AeroCom (Myhre et al., 2013), ACCMIP (Lamarque et al., 2013), and Arctic Monitoring and Assessment Programme (AMAP) Phase I (AMAP, 2011). Several recent updates of BC emissions suggest significant improvement over the abovementioned inventories. Hao et al. (2016) reported biomass burning emission in northern Eurasia was 3.2 times higher than reported by GFED version4 (GFED4). Huang, Fu, et al. (2015) and Huang, Song, et al. (2015) reassessed Russian anthropogenic BC emission, including gas flaring, as 0.224 Tg/year in 2010, which was 2 times greater than that reported by Bond et al. (2007). Huang and Fu (2016) developed a global gas flaring BC emission inventory of 0.13 Tg/year. In this study, we apply these updated inventories with the GEOS-Chem (v11-01) model to examine their reliability and also revisit the BC DRE with special focus on the Arctic region due to the significant absorbing effect of BC in high latitudes.

2. Methods

2.1. Emission Updates

In this section, we briefly compare the emission updates with the benchmark inventories commonly used by previous modeling efforts. The benchmark BC inventories refer to anthropogenic emission from Bond et al. (2007; hereafter referred to as BOND) and biomass burning from GFED4; the emission updates are described below.

The first emission update examined is Fire Emission Inventory for northern Eurasia (FEI-NE) of biomass burning emission from Hao et al. (2016) with updates over northern Eurasia (35–80°N, 10°W–170°E). Biomass burning emission is usually derived as the product of burned area, fuel loading, combustion completeness, and emission factor. Although there are several different inventories, such as Fire Inventory from NCAR (FINN) (Wiedinmyer et al., 2011), Fire Locating and Monitoring of Burning Emissions (FLAMBE) (Reid et al., 2009), GFED, and Quick Fire Emission Data (QFED) (Darmenov & da Silva, 2015), they all share similar methodology of utilizing satellites to locate fire activity and emission factors collected from field measurements; different algorithms are utilized to estimate other variables mentioned above. To estimate fuel loading, the FEI-NE inventory employed local fine-resolution (250 m) land cover and forest species information combined with satellite measurements, while the GFED used the satellite-driven biogeochemical model (van der Werf et al., 2010). FEI-NE applied an empirical fire effects model (Prichard et al., 2006) to calculate combustion completeness as a function of mass loading and moisture content of multiple fuel components, while GFED used combustion completeness values which were scaled with soil moisture between predefined upper and lower bounds. FEI-NE used the BC emission factor as 0.93 and 1.36 g/kg (May et al., 2014) for forest and nonforest (grassland/shrubland/savanna) burning, respectively; agricultural burning was not considered in FEI-NE inventory. However, emission factors from May et al. (2014) were compiled for flight campaigns in California and South Carolina, and also for laboratory-measured emission factors from open burning with 15 individual plant species commonly found in the United States, which may not be representative for northern Eurasia where land cover and plant species are both significantly different. GFED reported the overall carbon and dry matter emission only; in this study we applied the emission factors by Akagi et al. (2011) as 0.46 and 0.56 g/kg for savanna and deforestation/extratropical forest/peat/woodland, which is recommended by the GFED developers. As seen in Figures 1a and 1b, both the quantity and the spatial allocation differ prominently between FEI-NE and GFED4. In 2011 and 2012, FEI-NE emission was 613.5 and 941.3 Gg/year, respectively, while GFED4 was 105.3 and 203.3 Gg/year, respectively.

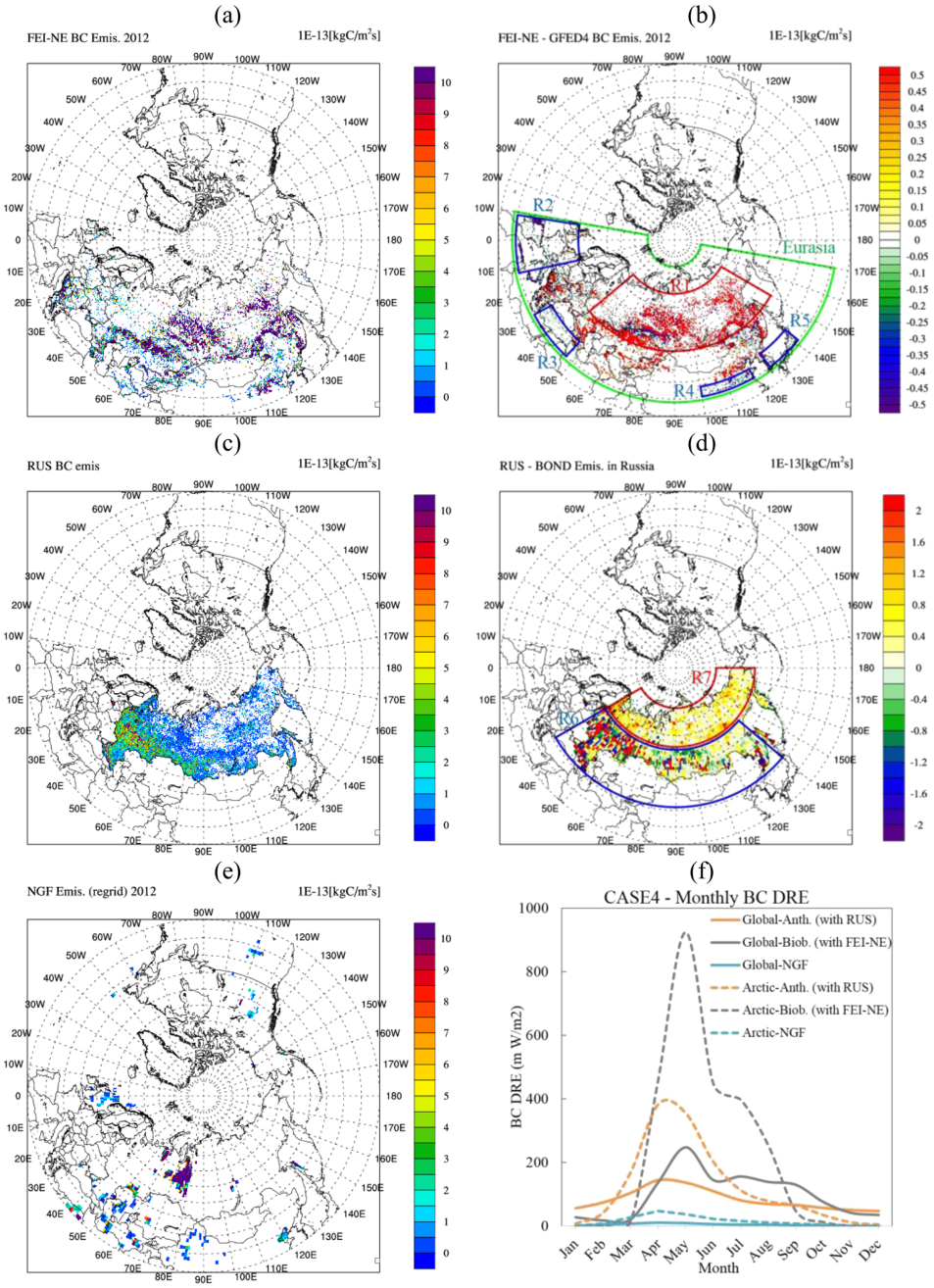

Figure 1. Spatial distributions of BC emission from the (a) FEI-NE inventory, (b) difference between FEI-NE and GFED over northern Eurasia, (c) RUS inventory, (d) difference between RUS and BOND over Russia, (e) Natural gas flaring inventory, and (f) zonal distributions of BC emission in 30–90°N (BOND emission is configured with the secondary axis). BC = black carbon; FEI-NE = Fire Emission Inventory-northern Eurasia; GFED = Global Fire Emission Database; RUS = RUssia.

Region R1 in Figure 1b denotes the area where FEI-NE was higher (50–70°N, 40–150°E), and areas where GFED4 was higher are indicated as regions R2 (35–55°N, 10°W–12°E), R3 (35–41°N, 28–47°E), R4 (35–38°N, 100–120°E), and R5 (35–39°N, 127–141°E).

The second emission update is anthropogenic emissions over Russia from Huang, Fu, et al. (2015) and Huang, Song, et al. (2015), hereafter referred to as RUS. As indicated by modeling studies (H. L. Wang, Rasch, et al., 2014) emission inventories from Russia are suspected to retain significant uncertainty due to limited documentation of activity and data. For example, the Office of Technological and Environmental

Surveillance of Russia reports BC emission factors of 1.1 and 6.1–7.1 g/kg for oil and coal-fueled power generation, respectively, while the emission factors summarized by Bond et al. (2004) were 0.04 and 0.002–0.009 g/kg, respectively. RUS applied the emission ratio between soot and total particulate matter (PM) to estimate the BC emission based on PM emission, where the ratio was collected from a recent measurement study conducted by the Scientific Research Institute for Atmospheric Air Protection in Russia (SRI-Atmosphere, 2012) and was believed to have a higher confidence level. RUS utilized more detailed and recently updated activity data, fuel consumption data, and on-site emission factor measurements, mostly collected from the local agencies, to construct the national level emission for Russia. BOND used a predefined percentage profile to categorize vehicles into five different types representing all countries in the former USSR with emission factors measured for U.S. vehicles (Yanowitz et al., 2000), while RUS categorized vehicles into a total of 27 types following Russia's transportation methodological guidelines and applied corresponding locally collected emission factors (Ministry of Transport of the Russian Federation Research Institute, MTRFRI, 2008). Spatial allocation for RUS applied district or provincial level activity data and socioeconomic indicators to map the emissions into a $0.1° \times 0.1°$ grid as shown in Figure 1c, while BOND estimated country-level emission which was primarily allocated based on population density within a $1° \times 1°$ grid. As seen in Figure 1d, both RUS and BOND estimated high emission in Moscow and the lower-latitude areas near Europe (R6, 41–60°N, 30–140°E) but with different spatial distribution, and RUS identified greater emissions in the remote areas of Siberia (R7, 61–75°N, 30–180°E) from industrial boilers and transport sectors.

The third emission update is global natural gas flaring (NGF) inventory from Huang and Fu (2016). Gas flaring was rarely considered as an emission source for BC prior to 2010 until pilot studies (Elvidge et al., 2016; Johnson et al., 2011) suggested that the incomplete combustion within flare stacks used in oil and gas production may generate a substantial amount of particulate. More research efforts have been devoted in recent years to measure the emissions from gas flaring facilities, but the reported emission factors vary significantly, even over the same campaign field. For example, two different measurement campaigns (Schwarz et al., 2015; Weyant et al., 2016) using identical single particle soot photometer (SP2) methods in the same location (Bakken oil-production field in north Dakota) reported an upper limit BC emission rate from 0.28 to 0.57 ± 0.14 g/m^3. This is because many dynamic factors such as operating practices, fuel gas flow rate, gas components, flame turbulence, and combustion conditions will affect combustion efficiency and, therefore, the production of BC. Measured BC emission factors may vary by a factor of 50 between different flares, even within the same oil and gas field (Weyant et al., 2016). Rather than applying a universal emission factor, NGF adopted an empirical method (Conrad & Johnson, 2017; McEwen & Johnson, 2012) to estimate the emission factor as a function of the volume-weighted heating value of associated petroleum gas (APG) composition with APG information collected from literature and compiled in a global database. Using gas flaring volumes derived from the NOAA Defense Meteorological Satellite Program (DMSP), the region-dependent emission factors were applied to estimate the quantity and spatial distribution of gas flaring emission. A zonal average distribution of the benchmark inventories and updates are shown in Figure 1e, demonstrating the substantial excess emissions indicated by these updates.

2.2. Simulation Configurations

We conducted a series of simulations with different sets of emission inputs to explicitly identify the changes of direct forcing due to emission updates. The simulated scenarios include the following: CASE1, simulation with benchmark BC emissions from GFED4 and BOND; CASE2, same as CASE1 but with biomass burning emission in northern Eurasia replaced by FEI-NE; CASE3, same as CASE2 but with anthropogenic emission in Russia replaced by RUS; and CASE4, same as CASE3 but with the global natural gas flaring emission from NGF included. Each scenario is simulated for years 2011 and 2012 with a 1-year spin-up to provide the initial conditions in GEOS-Chem. To quantify the BC DRF, we configured a preindustry simulation as 1850 with emission adopted from Dentener et al. (2006).

3. Results and Discussion

3.1. Emissions Uncertainties Indicated by Model Evaluation

Modeled results are compared with AAOD from Ozone Monitoring Instrument (OMI) and AERONET measurements, and with surface BC mass concentration observations collected from Arctic EBAS sites

(http://ebas.nilu.no/Default.aspx). Evaluation statistics are analyzed over the emission-updated areas to investigate their potential uncertainties.

Figure 2 presents the spatial distributions of annual average simulation bias for 2011 and the evaluation statistics (derived with monthly averages from 2011 and 2012). In general, both CASE1 and CASE2 show poor correlation (<0.5) with observations, but normalized mean bias (NMB) differs significantly between the two scenarios. Figures 2a and 2b suggest that CASE1 exhibits moderate bias against OMI over R1 and R2–R5 with NMB of −12% and 22%, respectively, while Figures 2e and 2f suggest that CASE2 substantially overestimates AAOD with NMB of 94% over R1 and 28% over R2–R5. Evaluation against AERONET also indicates overestimation of AAOD over R1 by CASE2 (90%), but suggests that both scenarios moderately underestimate AAOD over R2–R5 by ~20%. Over the whole northern Eurasia domain, CASE1 underestimates by 18% and CASE2 overestimates by 18% when compared with OMI observations, and CASE1 underestimates by 13% and CASE2 slightly overestimates by 0.4% when compared with AERONET observations. Over the Arctic and NH, CASE2 exhibits better performance for both AAOD and surface BC mass concentrations. Evangeliou et al. (2016) examined LMDz-OR-INCA model simulations at five Arctic observation sites and concluded that simulation using FEI-NE had substantially better agreement with observations than simulation using GFED3, but our study demonstrates that the FEI-NE inventory may overestimate biomass burning emission over northern Eurasia. Considering the burned area, fuel loading and combustion completeness were all characterized with local data, the BC emission factors derived from U.S. plant species may be responsible for the large overestimation of FEI-NE.

Figures 2c and 2g shows CASE3 performance. Evaluation with OMI suggests the NMB values over R6, R7, and Russia are 97%, 59%, and 67%, respectively, for CASE3, and 93%, 55%, and 63%, respectively, for CASE2. AERONET also suggests no significant difference between CASE3 and CASE2, indicating that applying the RUS inventory update shows no prominent impact on model performance in Russia. Using the GFED and BOND inventory, CASE1 underestimates AAOD over R6, R7, and Russia by 15–40%, indicating that the large positive bias in CASE2 and CASE3 is attributable to applying FEI-NE inventory in these scenarios. Evaluation over the Arctic and the NH shows even smaller differences between the two scenarios. Huang, Fu, et al. (2015) and Huang, Song, et al. (2015) reported that applying the RUS emission on top of EDGAR-HTAPv2 inventory substantially improved the AAOD underestimation over Russia, reducing NMB from −50% to −20%. But EDGAR-HTAP estimated BC emission in Russia was only 46 and 33 Gg in 2000 and 2010, respectively, significantly lower than BOND (130 Gg) and RUS (224 Gg including gas flaring).

Figures 2d and 2h demonstrates the CASE4 performance. No significant difference was found between CASE3 and CASE4 at the hemispheric scale; both scenarios underestimate AAOD by 5% and 8% when compared with OMI and AERONET, respectively. However, evaluation over the EBAS sites in the Arctic suggests a notable improvement in agreement between modeled and observed BC mass concentration, with correlation coefficients of 0.5 and 0.7 for CASE3 and CASE4, respectively, and NMB of −68% and − 57%, respectively. Over the source region, Huang and Fu (2016) validated the Hemispheric-CMAQ-simulated AAOD with MISR over the Urals Federal District, which hosts the majority flaring activities in Russia and reported NMB of −14%, but the evaluation excluded 20% of the data with large positive bias as outliers. Our evaluation, inclusive of outliers, suggests that CASE3 and CASE4 are closely comparable over Russia.

3.2. Estimates of BC DRE, DRF, and the Contributions From Different Emission Sectors

BC DRE at top of atmosphere (TOA) under all sky conditions estimated in CASE1 and CASE4 scenarios are presented in Figure 3. CASE4 estimated global average BC DRE and DRF is about 35% higher than CASE1, but 2 times that of CASE1 over the Arctic (data summarized in Table 1). The emission differs by only 10% between the two scenarios on the global scale, but most updates are located over high latitudes in northern Eurasia as shown in Figure 3f. For 30–90°N, BC emission employed by CASE4 (3.6 Tg/year) was 33% higher than that used by CASE1 (2.7 Tg/year). For 60–90°N, CASE4 emission (406 Gg/year) is ~3 times that of CASE1 (133 Gg/year), with most of the additional emissions contributed by FEI-NE and NGF. Comparison between the two scenarios suggests that the emission updates have significant meaning for revisiting the BC DRE and DRF, and the BC emission in higher latitudes is more efficiently absorbing (H. Wang et al., 2013), consistent with the findings from previous studies (AMAP, 2015; Shindell, 2012).

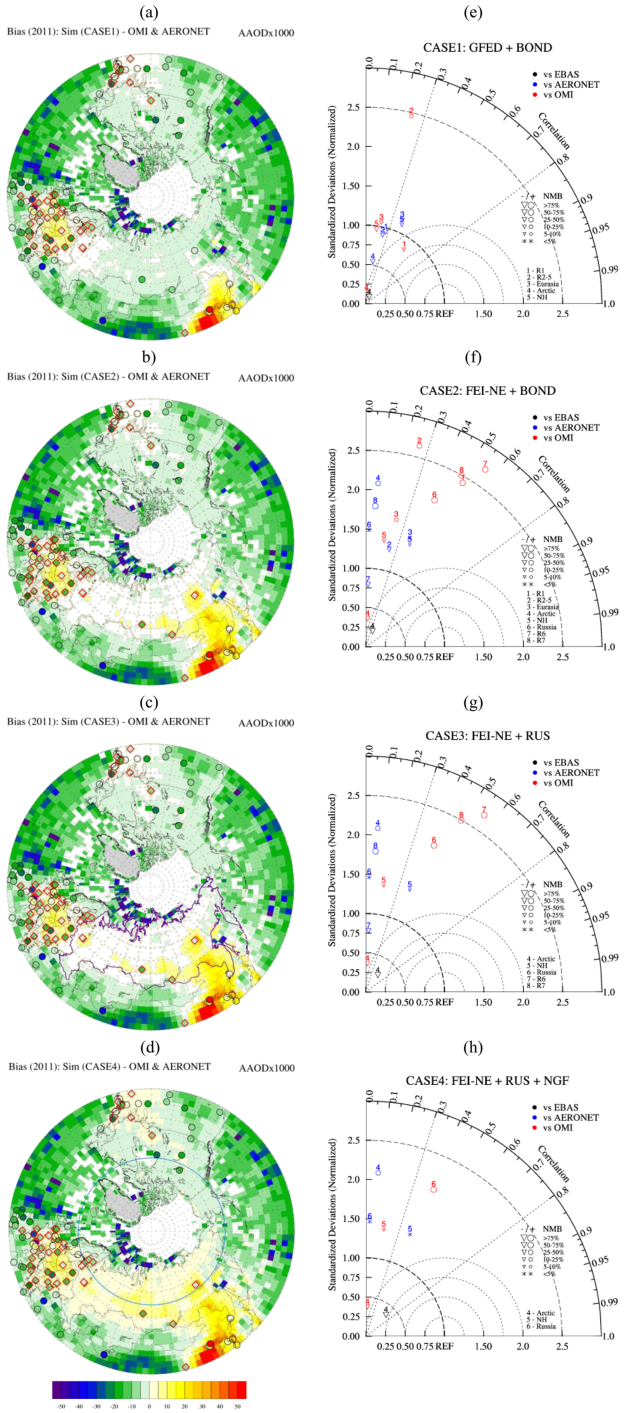

Figure 2. Spatial distributions of aerosol absorbing optical depth (AAOD) simulation bias against ozone monitoring instrument (OMI) and AErosol RObotic NETwork (AERONET) for year 2011 (left column) and Taylor diagrams of evaluation statistics against OMI, AERONET, and EBAS for year 2011 and 2012 (right column) under CASE1 (a, e), CASE2 (b, f), CASE3 (c, g), and CASE4 (d, h) scenarios. Note that in the spatial distribution figures AAOD and the biases were scaled by a factor of 1.000 as the raw numbers are too small. AERONET stations are indicated with markers, and the bias against AERONET is overlaid on top of the bias against OMI. Black circles indicate the consistent sign of bias between AERNET and OMI, and red diamonds indicate the opposite sign of bias. National boundary of Russia is highlighted in purple and boundary of Arctic is highlighted in blue. FEI-NE = Fire Emission Inventory-northern Eurasia; GFED = Global Fire Emission Database; RUS = RUssia.

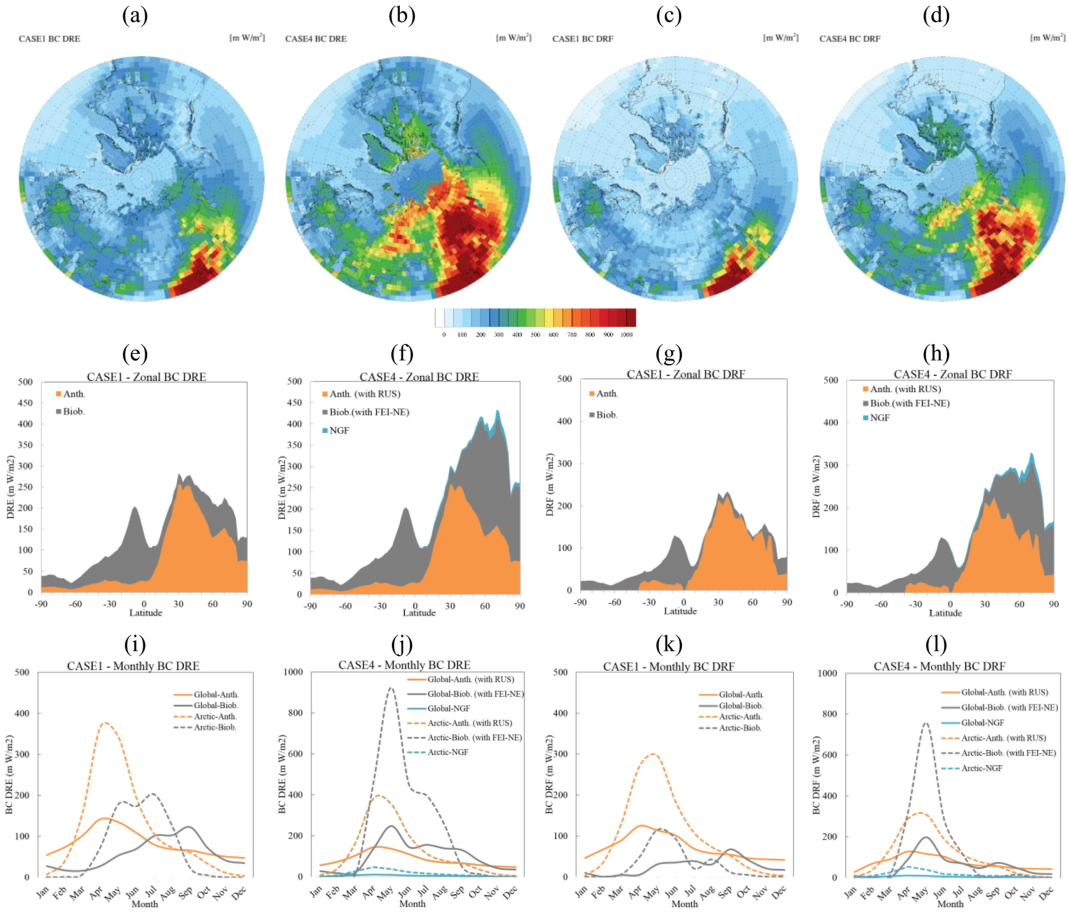

Figure 3. Estimations of black carbon direct radiative forcing, BC DRE (a, b, e, f, i, and j) and direct radiative effect, DRF (c, d, g, h, k, and l) under CASE1 (a, c, e. g. i, and k) and CASE4 (b, d, f, h, j, and l) scenarios presented in spatial distributions (top row), zonal averages (middle row), and monthly variations (bottom row).

Spatial distribution of DRE and DRF follows a similar pattern of emission updates, with most significant changes found over northern Eurasia. Interestingly, a substantial increase in BC DRE is also identified over Greenland and the northern Nunavut province of Canada although no emission updates are applied in these areas. NGF emission updates in the United States are mainly located in North Dakota and Wyoming, and updates in Canada are mainly located in Saskatchewan and Alberta (Figure 1e). These updates are not only relatively far from Greenland and northern Nunavut but also relatively small and hardly induces any noticeable impact on the forcing budget even over the source regions as seen in Figures 3b and 3d. Therefore, the enhanced BC forcing over these areas is attributed to long-range transport of BC from northern Eurasia. Trajectory analysis studies (Klonecki et al., 2003; Stohl, 2006) suggested that the constant potential temperature over the Arctic developed closed domes which created a transport barrier near 70°N. Figures 3a–3d also demonstrates that the excessive BC in northern Eurasia can hardly penetrate directly through the Arctic. BC emission from high-latitude areas in the NH travels along zonal directions across the Pacific and affects forcing in the upper western hemisphere.

The zonal distributions and monthly variations of BC DRE and DRF are also presented in Figure 3. In the CASE1 scenario, anthropogenic emission dominates the BC forcing in the Arctic, and biomass burning contributes only 30–40%. But in CASE4, emission updates drastically alter the zonal average BC forcing over 30–90°N, with more than 60% contributed by biomass burning and 3–5% contributed by gas flaring. Seasonality of BC forcing is also changed. On the global (Arctic) scale, applying the FEI-NE inventory moves the biomass burning forcing peak from September (July) to May and results in a 2(4) times higher direct forcing. The NGF forcing exhibits minor influence and smooth seasonality on the global scale but shows a prominent peak in April over the Arctic region.

Table 1
Global and Arctic Average of BC DRE and DRF in This Study and Other Studies

	DRE (mW/m^2)		DRF (mW/m^2)		Emission		
						Inventory	
Reference	Global	Arctic	Global	Arctic	Tg/year	Anth.	Biob.
CASE1 in this study	139 (82)	182 (116)	94 (71)	118 (104)	6.7 (4.6)	BOND	GFED4
CASE4 in this study	186 (88)	351 (137)	131 (76)	247 (120)	7.4 (4.8)	BOND[a]	GFED4[b]
Bond et al. (2011)	470 (400)	400d	—	—-	7.0 (4.4)	BOND[c]	GFED2
Bond et al. (2013)	880	—	710 (510)[d]	—	17 (10.6)[e]	Bond et al. (2013)[f]	
Schulz et al. (2006)	(290)	—	(250)[d]	—	9.4 (6.3)	BOND[g]	GFED
Myhre et al. (2013)	(200)	—	230 (180)[h]	—	7.6 (5.0)	Lamarque et al. (2010)[i]	
Samset et al. (2014)	—	—	170[d]	—	7.6 (5.0)	Lamarque et al. (2010)	
(AMAP, 2011)	—	120	—	—	7.6 (5.0)	Lamarque et al. (2010)	
(AMAP, 2015)	—	640	—	—	8.3 (6.0)	ECLIPSE[j]	GFED3
H. Wang, Rasch, et al. (2014)	—	210	—	—	7.6 (5.0)	Lamarque et al. (2010)	
X. Wang, Heald, et al. (2014)	140 (80)	—	130 (80)[d]	—	6.9 (4.9)	BOND	GFED3[k]
Q. Wang, Jacob, et al. (2014)	—	—	190[l]	—	6.5 (4.9)	BOND[m]	GFED3

Note. Bracketed values are anthropogenic/industrial only for each value. BC = black carbon; DRF = direct radiative forcing; DRE = direct radiative effect; GFED = Global Fire Emission Database;
[a]With updates from Russia and natural gas flaring. [b]With updates from Fire Emission Inventory-northern Eurasia. [c]The mode input emission was from Bond et al. (2007) as 4.4 Tg/year for year 2000, and BOND used in this study was scaled by GEOS-Chem as 4.6 Tg/year for 2011 and 2012. [d]Preindustry simulation was configured as 1750 with 1.4 Tg/year BC emission from biofuel and biomass burning. [e]Emission inputs for model is 4.8 Tg/year and 2.8 Tg/year from anthropogenic and biomass burning, respectively, and the total estimated emission is upscaled to be 17 Tg/year after matching model result with observations. [f]Biomass burning emission was compiled from RETRO (Schultz et al., 2008) and GFED2. [g]Anthropogenic emission was based on Bond et al. (2004) but scaled with emission factors from IIASA/RAINS (Cofala et al., 2006). [h]Some of the AEROCOM phase II participating models configured preindustry simulation as 1,750 with emission from Dentener et al. (2006), while the rest of the models configured preindustry as 1850 with emission from Lamarque et al. (2010), which derived the 1850 emission based on EDGAR-HYDE (van Aardenne et al., 2001). [i]Lamarque et al. (2010) BC inventory for year 2000 was compiled from BOND and GFED2. [j]The Arctic Monitoring and Assessment Programme (AMAP) Phase II program (AMAP, 2015) applied both ECLIPSEv4a and v5 (Klimont et al., 2017) for modeling, but the forcing was estimated with simulation from v4a. [k]H. Wang, Rasch, et al. (2014) applied 12-year (2000–2011) average of GFED3 to represent for 2010. [l]This study did not describe the preindustry configuration. [m]Anthropogenic emission in Russia was doubled to match model simulation with local AErosol RObotic NETwork observations, anthropogenic emission in Asia was replaced with Zhang et al. (2009) which was 50% higher than BOND, North American emissions was decreased by 30% to match model with observations, and aviation emission was from Simone et al. (2013).

3.3. Comparison With Other Studies

Table 1 compares DRE and DRF between our study and some of the most frequently cited studies and the emission inventories employed, including contributions by source type, if available. The reported estimations vary significantly among these studies, by a factor of 6 and 5 for global and Arctic, respectively. The largest estimates were reported by Bond et al. (2013) because the emission was scaled from 7.4 to 17 Tg/year to match model simulated AAOD with AERONET observations. The scaled estimates almost doubled an earlier assessment with the same baseline emission inputs conducted by Bond et al. (2011). Through AeroCom Phase I and II multimodel studies, Schulz et al. (2006) and Myhre et al. (2013) reported global DRE and DRF due to anthropogenic emission that were about 3 times greater than our estimation. An important implication is that although AeroCom Phase II applied a higher emission inventory, simulated DRE and DRF was 50% lower than Phase I due to updated model parameterizations and inclusion of more participating models. Samset et al. (2014) applied aircraft observations to constrain the AeroCom Phase II outputs and reported an even lower DRF of 170 mW/m^2 after scaling. With special focus on Arctic region through the AMAP Phase I program, AMAP (2011) reported BC DRE over the Arctic as 120 mW/m^2. However, AMAP Phase II, with slightly increased emission (10%), reported that DRE was 5 times greater than the previous estimation (AMAP, 2015), close to estimations by Flanner et al. (2009). Applying the same emission inventory, H. Wang, Rasch, et al. (2014) reported that BC DRE in the Arctic was almost 2 times that of the AMAP Phase I estimation. Our estimations generally fall within the lower bound of the 50–800 mW/m^2 range of IPCC AR5. AMAP (2015) estimated Russian flaring BC generated 26 mW/m^2 DRE in the Arctic by modeling with the ECLIPSE emission inventory (Klimont et al., 2017), compared with our estimation of 15 mW/m^2. The difference is attributed to both the emissions (ECLIPSE flaring is 226 Gg/year, 70% higher than NGF) and the models applied.

Most of the studies in Table 1 employed similar emission data sets, with anthropogenic inventories from Bond et al. (2004) or Bond et al. (2007) and biomass burning inventories from different versions of GFED, except that the AMAP Phase II used anthropogenic emissions from ECLIPSE. By comparing the CASE1 and CASE4 scenarios, we have found that the emission updates in Eurasia can lead to substantial enhancement of Arctic forcing estimates because northern Eurasia is the largest contributor (AMAP, 2015; Qi et al., 2017). If we apply the regional temperature potential (RTP) coefficient promoted by Shindell (2012), direct forcing caused by BC will lead to a 0.14 and 0.27 °C equilibrium temperature rise in the Arctic based on estimates from CASE1 and CASE4, respectively. Considering the climate responses induced by BC-in-snow, the influence of high-latitude emission may play an even more important role than previously expected.

4. Summary and Conclusions

The goal of this study was to evaluate some of the recent BC emission updates in high-latitude areas and evaluate their impacts on estimation of direct forcing. We focused on comparing simulation performance in the source regions, Arctic, and on the NH scale to portray potential uncertainties within the updated inventories. We then compared our estimations of BC DRE and DRF with other recent studies.

No simple preference could be concluded regarding these emission updates except for NGF. Theoretically, all of the updates are expected to better describe the emission intensity and spatial distribution, but the modeled results, as evaluated against observations, do not show prominent supportive performance. As compared to GFED4, applying the FEI-NE inventory changes negative bias to positive bias, but generally of the same magnitude. Although applying updated emission shows better performance in the Arctic, it may not be considered as a solid demonstration because most previous modeling efforts underestimate surface BC in the Arctic. The FEI-NE inventory might be overestimated in the source region due to employing emission factors for northern Eurasia that were determined from U.S. vegetation and land use data. The RUS inventory (excluding gas flaring in Russia) is close to BOND but has different spatial distribution, yet the $2° \times 2.5°$ GEOS-Chen grid resolution in this study results in very similar performance; therefore, we recommend fine-grid modeling efforts with regional models to further distinguish between these inventories. Applying the NGF inventory improved model performance in the Arctic, without introducing excessive surface BC over the source regions; it is therefore recommended that it be included in future modeling efforts. However, a detailed comparison between NGF and ECLIPSE is necessary as they are developed with different methodologies and vary by 70%.

We have found that comprehensive evaluation incorporating multiple data sets from different platforms is necessary to reveal the reasonable performance of models and uncertainty of emission inventories. Many previous modeling studies suggested underestimation of simulated BC over the Arctic region and upscaled the emission to match the simulation with observations, but the simulation biases in the remote sites are attributed to the net effect of uncertainties inherited from both the emission inventory and model parameterization. A higher emission input such as FEI-NE may help to drive simulated BC mass and AAOD over the Arctic sites closer to observations, but it may not help narrow down the remaining uncertainties. The major limitation of this study is that the one-way GEOS-Chem model is unable to estimate the exact climate response to BC with inline mode. Therefore, we recommend applying two-way-mode models to further evaluate how the recently reported emission inventories may update our understanding of the BC impacts on climate. Finally, our findings suggest an urgent need to improve the reliability of emission inventories in the high latitudes, especially over Eurasia due to its influential contribution to the Arctic. Research efforts such as applying locally collected emission factors with plant species representing northern Eurasia should be devoted in the future study to narrow down the remaining emission inventory uncertainties.

Acknowledgments
We greatly thank the Joint Institute for Computational Sciences of the University of Tennessee and Oak Ridge National Laboratory for providing the computational resources used in this research. This work is supported by Interagency Acquisition Agreement S-OES-11_IAA-0027 from the U.S. Department of State to the U.S. Department of Energy. K. H is supported by the National Natural Science Foundation of China (41429501, 91644105) and Funds for International Cooperation and Exchange of Shanghai Science and Technology Commission (18230722600). We also appreciate the help from Christopher Holmes for correcting a bug associated with RRTMG in GEOS-Chem model v11-01. The AERONET data can be reached here: https://aeronet.gsfc.nasa.gov/new_web/data.html; the EBAS data can be downloaded from https://ebas.nilu.no/; the OMI data are available at https://mirador.gsfc.nasa.gov/; the FEI-NE inventory can be obtained via https://www.fs.usda.gov/rds/archive/Product/RDS-2016-0036/; and the RUS and NGF inventories are available at http://acs.engr.utk.edu/Data.php.

References

Akagi, S. K., Yokelson, R. J., Wiedinmyer, C., Alvarado, M. J., Reid, J. S., Karl, T., et al. (2011). Emission factors for open and domestic biomass burning for use in atmospheric models. *Atmospheric Chemistry and Physics*, *11*(9), 4039–4072. https://doi.org/10.5194/acp-11-4039-2011

AMAP (2011). *The impact of black carbon on Arctic climate*. Oslo, Norway: AMAP.

AMAP (2015). *AMAP assessment 2015: Black carbon and ozone as Arctic climate forcers*. Oslo, Norway: AMAP.

Bond, T. C., Bhardwaj, E., Dong, R., Jogani, R., Jung, S., Roden, C., et al. (2007). Historical emissions of black and organic carbon aerosol from energy-related combustion, 1850–2000. *Global Biogeochemical Cycles*, *21*, GB2018. https://doi.org/10.1029/2006GB002840

Bond, T. C., Doherty, S. J., Fahey, D. W., Forster, P. M., Berntsen, T., DeAngelo, B. J., et al. (2013). Bounding the role of black carbon in the climate system: A scientific assessment. *Journal of Geophysical Research: Atmospheres*, *118*, 5380–5552. https://doi.org/10.1002/jgrd.50171

Bond, T. C., Streets, D. G., Yarber, K. F., Nelson, S. M., Woo, J. H., & Klimont, Z. (2004). A technology-based global inventory of black and organic carbon emissions from combustion. *Journal of Geophysical Research*, *109*, D14203. https://doi.org/10.1029/2003JD003697

Bond, T. C., Zarzycki, C., Flanner, M. G., & Koch, D. M. (2011). Quantifying immediate radiative forcing by black carbon and organic matter with the Specific Forcing Pulse. *Atmospheric Chemistry and Physics*, *11*, 1505–1525. https://doi.org/10.5194/acp-11-1505-2011

Cofala, J., Amann, M., & Mechler, R. (2006). *Scenarios of global anthropogenic emissions of air pollutants and methane up to 2030*. Laxenburg, Austria: International Institute for Applied Systems Analysis (IIASA). Retrieved from https://www.iiasa.ac.at/rains/global_emiss/IR-06--023.pdf

Conrad, B. M., & Johnson, M. R. (2017). Field measurements of black carbon yields from gas flaring. *Environmental Science & Technology*, *51*(3), 1893–1900.

Darmenov, A., & da Silva, A. (2015). The quick fire emissions dataset (QFED): Documentation of versions 2.1, 2.2 and 2.4, NASA Technical Report Series on Global Modeling and Data Assimilation, NASA TM-2015-104606 (Vol. 38). Retrieved from https://gmao.gsfc.nasa.gov/pubs/docs/Darmenov796.pdf

Dentener, F., Kinne, S., Bond, T., Boucher, O., Cofala, J., Generoso, S., et al. (2006). Emissions of primary aerosol and precursor gases in the years 2000 and 1750 prescribed data-sets for AeroCom. *Atmospheric Chemistry and Physics*, *6*(12), 4321–4344. https://doi.org/10.5194/acp-6-4321-2006

Elvidge, C. D., Zhizhin, M., Baugh, K., Hsu, F. C., & Ghosh, T. (2016). Methods for global survey of natural gas flaring from visible infrared imaging radiometer suite data. *Energies*, *9*(1), 14. https://doi.org/10.3390/en9010014

Evangeliou, N., Balkanski, Y., Hao, W. M., Petkov, A., Silverstein, R. P., Corley, R., et al. (2016). Wildfires in northern Eurasia affect the budget of black carbon in the Arctic—A 12-year retrospective synopsis (2002–2013). *Atmospheric Chemistry and Physics*, *16*(12), 7587–7604. https://doi.org/10.5194/acp-16-7587-2016

Flanner, M. G., Zender, C. S., Hess, P. G., Mahowald, N. M., Painter, T. H., Ramanathan, V., & Rasch, P. J. (2009). Springtime warming and reduced snow cover from carbonaceous particles. *Atmospheric Chemistry and Physics*, *9*(7), 2481–2497.

Hao, W. M., Petkov, A., Nordgren, B. L., Corley, R. E., Silverstein, R. P., Urbanski, S. P., et al. (2016). Daily black carbon emissions from fires in northern Eurasia for 2002-2015. *Geoscientific Model Development*, *9*(12), 4461–4474.

Heald, C. L., Ridley, D. A., Kroll, J. H., Barrett, S. R. H., Cady-Pereira, K. E., Alvarado, M. J., & Holmes, C. D. (2014). Contrasting the direct radiative effect and direct radiative forcing of aerosols. *Atmospheric Chemistry and Physics*, *14*, 5513–5527. https://doi.org/10.5194/acp-14-5513-2014

Huang, K., & Fu, J. S. (2016). A global gas flaring black carbon emission rate dataset from 1994 to 2012. *Scientific Data*, *3*, 160104. https://doi.org/10.1038/sdata.2016.104

Huang, K., Fu, J. S., Prikhodko, V. Y., Storey, J. M., Romanov, A., Hodson, E. L., et al. (2015). Russian anthropogenic black carbon: Emission reconstruction and Arctic black carbon simulation. *Journal of Geophysical Research: Atmospheres*, *120*, 11,306–11,333. https://doi.org/10.1002/2015JD023358

Huang, X., Song, Y., Zhao, C., Cai, X. H., Zhang, H. S., & Zhu, T. (2015). Direct radiative effect by multicomponent aerosol over China. *Journal of Climate*, *28*(9), 3472–3495.

Huneeus, N., Schulz, M., Balkanski, Y., Griesfeller, J., Prospero, J., Kinne, S., et al. (2011). Global dust model intercomparison in AeroCom phase I. *Atmospheric Chemistry and Physics*, *11*(15), 7781–7816. https://doi.org/10.5194/acp-11-7781-2011

Johnson, M. R., Devillers, R. W., & Thomson, K. A. (2011). Quantitative field measurement of soot emission from a large gas flare using sky-LOSA. *Environmental Science & Technology*, *45*(1), 345–350.

Klimont, Z., Kupiainen, K., Heyes, C., Purohit, P., Cofala, J., Rafaj, P., et al. (2017). Global anthropogenic emissions of particulate matter including black carbon. *Atmospheric Chemistry and Physics*, *17*(14), 8681–8723. https://doi.org/10.5194/acp-17-8681-2017

Klonecki, A., Hess, P., Emmons, L., Smith, L., Orlando, J., & Blake, D. (2003). Seasonal changes in the transport of pollutants into the Arctic troposphere-model study. *Journal of Geophysical Research*, *108*(D4), 8367. https://doi.org/10.1029/2002JD002199

Lamarque, J. F., Bond, T. C., Eyring, V., Granier, C., Heil, A., Klimont, Z., et al. (2010). Historical (1850–2000) gridded anthropogenic and biomass burning emissions of reactive gases and aerosols: Methodology and application. *Atmospheric Chemistry and Physics*, *10*(15), 7017–7039. https://doi.org/10.5194/acp-10-7017-2010

Lamarque, J. F., Shindell, D. T., Josse, B., Young, P. J., Cionni, I., Eyring, V., et al. (2013). The Atmospheric Chemistry and Climate Model Intercomparison Project (ACCMIP): Overview and description of models, simulations and climate diagnostics. *Geoscientific Model Development*, *6*(1), 179–206. https://doi.org/10.5194/gmd-6-179-2013

May, A. A., McMeeking, G. R., Lee, T., Taylor, J. W., Craven, J. S., Burling, I., et al. (2014). Aerosol emissions from prescribed fires in the United States: A synthesis of laboratory and aircraft measurements. *Journal of Geophysical Research: Atmospheres*, *119*, 11,826–11,849. https://doi.org/10.1002/2014JD021848

McEwen, J. D. N., & Johnson, M. R. (2012). Black carbon particulate matter emission factors for buoyancy-driven associated gas flares. *Journal of the Air & Waste Management Association*, *62*(3), 307–321.

Ministry of Transport of the Russian Federation Research Institute (MTRFRI) (2008). Ministry of Transport of the Russian Federation Research Institute, Instructions on the inventory of emissions of motor vehicles into the air (in Russian). Расчетная инструкция (методика) по инвентаризации выбросов загрязняющих веществ автотранспортными средствами в атмосферный воздух.

Myhre, G., Samset, B. H., Schulz, M., Balkanski, Y., Bauer, S., Berntsen, T. K., et al. (2013). Radiative forcing of the direct aerosol effect from AeroCom phase II simulations. *Atmospheric Chemistry and Physics*, *13*(4), 1853–1877. https://doi.org/10.5194/acp-13-1853-2013

Prichard, S. J., Ottmar, R. D., and Anderson, G. K. (2006). Consume 3.0 user's guide (234 pp.). Corvallis, OR: Pacific Northwest Research Station. Retrieved from https://www.fs.fed.us/pnw/fera/research/smoke/consume/consume30_users_guide.pdf, accessed on November 29, 2016.

Qi, L., Li, Q. B., Henze, D. K., Tseng, H. L., & He, C. L. (2017). Sources of springtime surface black carbon in the Arctic: An adjoint analysis for April 2008. *Atmospheric Chemistry and Physics*, *17*(15), 9697–9716.

Reid, J. S., Hyer, E. J., Prins, E. M., Westphal, D. L., Zhang, J., Wang, J., et al. (2009). Global monitoring and forecasting of biomass-burning smoke: Description of and lessons from the fire locating and modeling of burning emissions (FLAMBE) program. *IEEE Journal of Selected Topics in Applied Earth Observations and Remote Sensing*, *2*(3), 144–162. https://doi.org/10.1109/JSTARS.2009.2027443

Samset, B. H., & Myhre, G. (2015). Climate response to externally mixed black carbon as a function of altitude. *Journal of Geophysical Research: Atmospheres*, *120*, 2913–2927. https://doi.org/10.1002/2014JD022849

Samset, B. H., Myhre, G., Herber, A., Kondo, Y., Li, S. M., Moteki, N., et al. (2014). Modelled black carbon radiative forcing and atmospheric lifetime in AeroCom phase II constrained by aircraft observations. *Atmospheric Chemistry and Physics*, *14*(22), 12,465–12,477. https://doi.org/10.5194/acp-14-12465-2014

Schultz, M. G., Heil, A., Hoelzemann, J. J., Spessa, A., Thonicke, K., Goldammer, J. G., et al. (2008). Global wildland fire emissions from 1960 to 2000. *Global Biogeochemical Cycles*, *22*, GB2002. https://doi.org/10.1029/2007GB003031

Schulz, M., Textor, C., Kinne, S., Balkanski, Y., Bauer, S., Berntsen, T., et al. (2006). Radiative forcing by aerosols as derived from the AeroCom present-day and pre-industrial simulations. *Atmospheric Chemistry and Physics*, *6*(12), 5225–5246. https://doi.org/10.5194/acp-6-5225-2006

Schwarz, J. P., Holloway, J. S., Katich, J. M., McKeen, S., Kort, E. A., Smith, M. L., et al. (2015). Black carbon emissions from the Bakken oil and gas development region. *Environmental Science & Technology Letters*, *2*(10), 281–285. https://doi.org/10.1021/acs.estlett.5b00225

Shindell, D. T. (2012). Evaluation of the absolute regional temperature potential. *Atmospheric Chemistry and Physics*, *12*(17), 7955–7960.

Simone, N. W., Stettler, M. E. J., & Barrett, S. R. H. (2013). Rapid estimation of global civil aviation emissions with uncertainty quantification. *Transportation Research Part D: Transport and Environment*, *25*, 33–41. https://doi.org/10.1016/j.trd.2013.07.001

SRI-Atmosphere (2012). Review of existing method for assessment of emissions (PM/soot) used in Russia for major sources. Chapter 3.1. Calculation methods used in Russia to estimate PM/soot emissions from power plants and boilers (in Russian), St. Petersburg, 2012.

Stohl, A. (2006). Characteristics of atmospheric transport into the Arctic troposphere. *Journal of Geophysical Research*, *111*, D11306. https://doi.org/10.1029/2005JD006888

Tosca, M. G., Randerson, J. T., & Zender, C. S. (2013). Global impact of smoke aerosols from landscape fires on climate and the Hadley circulation. *Atmospheric Chemistry and Physics*, *13*(10), 5227–5241.

van Aardenne, J. A., Dentener, F. J., Olivier, J. G. J., Klein Goldewijk, C. G. M., & Lelieveld, J. (2001). A 1 × 1 degree resolution dataset of historical anthropogenic trace gas emissions for the period 1890–1990. *Global Biogeochemical Cycles*, *15*, 909–928. https://doi.org/10.1029/2000GB001265

van der Werf, G. R., Randerson, J. T., Giglio, L., Collatz, G. J., Mu, M., Kasibhatla, P. S., et al. (2010). Global fire emissions and the contribution of deforestation, savanna, forest, agricultural, and peat fires (1997–2009). *Atmospheric Chemistry and Physics*, *10*(23), 11,707–11,735. https://doi.org/10.5194/acp-10-11707-2010

van der Werf, G. R., Randerson, J. T., Giglio, L., van Leeuwen, T. T., Chen, Y., Rogers, B. M., et al. (2017). Global fire emissions estimates during 1997–2016. *Earth System Science Data*, *9*(2), 697–720. https://doi.org/10.5194/essd-9-697-2017

Wang, H., Easter, R. C., Rasch, P. J., Wang, M., Liu, X., Ghan, S. J., et al. (2013). Sensitivity of remote aerosol distributions to representation of cloud-aerosol interactions in a global climate model. *Geoscientific Model Development*, *6*(3), 765–782. https://doi.org/10.5194/gmd-6-765-2013

Wang, H. L., Rasch, P. J., Easter, R. C., Singh, B., Zhang, R., Ma, P.-L., et al. (2014). Using an explicit emission tagging method in global modeling of source-receptor relationships for black carbon in the Arctic: Variations, sources, and transport pathways. *Journal of Geophysical Research: Atmospheres*, *119*, 12,888–12,909. https://doi.org/10.1002/2014JD022297

Wang, Q., Jacob, D. J., Spackman, J. R., Perring, A. E., Schwarz, J. P., Moteki, N., et al. (2014). Global budget and radiative forcing of black carbon aerosol: Constraints from pole-to-pole (HIPPO) observations across the Pacific. *Journal of Geophysical Research: Atmospheres*, *119*, 195–206. https://doi.org/10.1002/2013JD020824

Wang, R., Andrews, E., Balkanski, Y., Boucher, O., Myhre, G., Samset, B. H., et al. (2018). Spatial representativeness error in the ground-level observation networks for black carbon radiation absorption. *Geophysical Research Letters*, *45*, 2106–2114. https://doi.org/10.1002/2017GL076817

Wang, X., Heald, C. L., Ridley, D. A., Schwarz, J. P., Spackman, J. R., Perring, A. E., et al. (2014). Exploiting simultaneous observational constraints on mass and absorption to estimate the global direct radiative forcing of black carbon and brown carbon. *Atmospheric Chemistry and Physics*, *14*(20), 10,989–11,010. https://doi.org/10.5194/acp-14-10989-2014

Weyant, C. L., Shepson, P. B., Subramanian, R., Cambaliza, M. O. L., Heimburger, A., McCabe, D., et al. (2016). Black carbon emissions from associated natural gas flaring. *Environmental Science & Technology*, *50*(4), 2075–2081. https://doi.org/10.1021/acs.est.5b04712

Wiedinmyer, C., Akagi, S. K., Yokelson, R. J., Emmons, L. K., Al-Saadi, J. A., Orlando, J. J., & Soja, A. J. (2011). The Fire INventory from NCAR (FINN): A high resolution global model to estimate the emissions from open burning. *Geoscientific Model Development*, *4*(3), 625–641.

Yanowitz, J., McCormick, R. L., & Graboski, M. S. (2000). In-use emissions from heavy-duty diesel vehicles. *Environmental Science & Technology*, *34*(5), 729–740.

Zhang, Q., Streets, D. G., Carmichael, G. R., He, K. B., Huo, H., Kannari, A., et al. (2009). Asian emissions in 2006 for the NASA INTEX-B mission. *Atmospheric Chemistry and Physics*, *9*(14), 5131–5153.